7-1-2016

IMPACTS OF WATER AND SALINE BRINE FLOW ON FRACTURED WELLBORE CEMENT

Joshua Robert Ellison

Joshua Ellison

Candidate

Civil Engineering

Department

This thesis is approved, and it is acceptable in quality and form for publication:

Approved by the Thesis Committee:

John Stormont, PhD, PE, Chairperson

Jose Cerrato, PhD

Eric Peterson, PhD

IMPACTS OF WATER AND SALINE BRINE FLOW ON FRACTURED WELLBORE CEMENT

by

JOSHUA ROBERT ELLISON

B.S., CIVIL ENGINEERING, UNIVERSITY OF NEW MEXICO, 2014

THESIS

Submitted in Partial Fulfillment of the
Requirements for the Degree of

Master of Science
Civil Engineering

The University of New Mexico
Albuquerque, New Mexico

May, 2016

Dedication

This is dedicated to my mother who made me promise her I would finish college when I stumbled early in my life.

Acknowledgements

Many individuals contributed to the completion of this thesis and I am sincerely thankful for each and everyone one.

To my committee, Dr. John Stormont, Dr. Jose Cerrato, and Dr. Eric Peterson, the advice, suggestions, expertise, and the unique knowledge you shared with me on this journey has reshaped the way I think. Your guidance has helped me to improve the way I articulate a technical argument. To my adviser, Dr. John Stormont, it was your words and your belief in me that persuaded me to pursue a master's degree and I will forever have the utmost respect for you.

To my fellow Master of Science candidate, Nabil Shaikh, you have undoubtedly proven to be one of the most talented people I have ever met. Your sound knowledge and expertise on the scanning electron microscope is just one of your resounding traits that I had the privilege to enjoy.

To my fellow Lobos, Omar, Savannah, Rashid, Tim, Shreya, Rahul, Moneeb, Laxmi, and Lauren, we shared our moments of success, failures, struggles, and laughter as we kept fighting the good fight. The many times we shared at Brickyard Pizza over a slice and a brew will always be one of my favorite memories. I wish you all the best in your future as we will undoubtedly go our separate ways.

To my parents, though you never quite understood what I was rambling about you continually assured me that I was strong enough, and smart enough to get through the challenges I faced both outside and inside my academics. Your unwavering love and support is a key reason why I kept chugging along. I hoped that I could somehow repay you for the many years you have taught and raised me to get through this life.

To my sister, Crystal, for innumerable conversations and long late-night phone calls we shared as we were both pursuing first our bachelor's degree, and then our master's. You, miss, constantly fueled me with motivation and kept me focused on the reasons why I needed to complete the journey. I love you dearly.

To my wife, Alyssa, and kids, Isaiah and Jayda, it was you three I always had in mind. You were my reason to start college, you three were my reason to continue college, and you three are the reason I finished college. Thank you for being understanding and allowing me to dedicate so much of my time to school. To my wife, Alyssa, your selflessness, patience, and care to carry our family as I spent six years on this journey has been the most respectable displays of love I have ever witnessed. You are a special woman that I have the honor to call my wife and I am forever grateful.

Last and most important, to my God and Savior, You blessed me with all of these people through Your grace and unparalleled love. All to Your glory.

Funding for this research was provided by the UNM Center for Water and the Environment, an NSF funded Center for Research Excellence in Science and Technology (Crest), NSF Award #1345169

IMPACTS OF WATER AND SALINE BRINE FLOW ON FRACTURED WELLBORE CEMENT

by

JOSHUA ROBERT ELLISON

B.S., CIVIL ENGINEERING, UNIVERSITY OF NEW MEXICO, 2014

M.S. CIVIL ENGINEERING, UNIVERSITY OF NEW MEXICO, 2016

Abstract

Fractures in wellbore cements can develop and provide pathways allowing fluids such as hydrocarbons or brines to communicate with freshwater aquifers and/or reach the surface. Once formed, these fractures can be altered by the stresses acting on them as well as reactions with the fluids moving through them. Previous studies, mostly with acidic brines flowing through a fracture, have shown dissolution/precipitation reactions cause permeability to decrease and mechanical properties to change as the acidic brine creates reaction fronts slowly propagate through the face of the fractures.

This study investigated fractured cement reacted with de-ionized water and saline brine under varying stress conditions. These fluids also contact carbon steel that was used to represent interaction with a steel casing within a wellbore. Flow measurements were made on a fractured cement core using nitrogen gas, de-ionized water, and saline brine under confining stresses up to 16.5 MPa. Flow through the fractured cement samples are interpreted as effective hydraulic aperture. After the flow measurements,

fracture surfaces were examined with X-ray diffraction analysis, scanning electron microscopy (SEM)/ energy dispersive X-ray spectroscopy (EDX), and inductively coupled plasma-optical emission spectroscopy (ICP-OES). Hardness values of reacted and unreacted cement fractures were measured.

The hydraulic aperture measured with nitrogen flow decreased in response to the initial increase in stress applied to the fracture due to crushing of asperities. Subsequent stress changes while flowing nitrogen through the fracture produced recoverable changes in the hydraulic aperture. De-ionized water flow through the fracture irreversibly reduced the hydraulic aperture by about 20% compared to nitrogen, attributable to the dissolution of portlandite which reduces the stiffness of the cement adjacent to the fracture surface and allows for additional closure of the fracture. During flow of saline brine, the hydraulic aperture progressively decreased and eventually approached that expected for intact cement. This so-called "self-healing" is attributed to (1) decreased fracture aperture from dissolution of portlandite, and (2) precipitation of calcite along the flow path.

Similar to many studies in this area of research, this study investigated the behavioral changes in fractured cement as it reacts with different fluids and is exposed to varying levels of confining stress. However, the physical and chemical impacts from brine that is not highly acidic are uniquely characterized to better understand what can be expected when fractured wellbores penetrate a saline aquifer.

Table of Contents

List of Figures

List of Tables

Chapter 1

Background

1.1 Problem Significance

Fractures in wellbore cements can develop and provide pathways allowing fluids such as hydrocarbons or brines to communicate with freshwater aquifers and/or reach the surface [Wiprut and Zoback, 1999; Zhang and Bachu, 2011; Dusseault et al., 2000]. This compromises the principal function of wellbore cement: to provide isolation between different formations penetrated by the wellbore. Fractured wellbore cement has led to the leaking of methane into the atmosphere, and older wellbores have proven to be especially vulnerable [Brufato et al., 2003]. At the end of 2015 a single well was responsible for leaking over 97,100 metric tons of methane into the atmosphere in Los Angeles, California. This volume was equal to 24% of all methane emissions in the Los Angeles Basin [Conley et al., 2016]. Also, fractures in wellbores have been identified as a pathway for saline flowback waters from hydrofracturing operations appearing in overlying freshwater aquifers [Haluszczack et al., 2013]. Wells used for CO_2 sequestration provide a direct connection from the CO_2 storage reservoir to freshwater aquifers and the atmosphere [Gasda et al., 2004].

Behavior of fractures in response to changes in environmental conditions (i.e. stress, fluid flow, chemical constituents in both solid and fluids) are not well understood, and repairing them can be difficult, time consuming, and can result in termination of use [Carey et al., 2010; Heathman and East, 1992]. Tens of thousands of wells are used for

oil and natural gas recovery, and according to the United States Energy Information Administration, the cost for drilling a single well is approximately 4 million US dollars [U.S. EIA, 2015]. Wellbores are expensive to construct/repair, can develop leakage pathways, may contaminate freshwater, and behavior of fractures in their cement is not well understood. Consequently, there is a strong motivation for better understanding of physical-chemical changes in wellbore systems.

1.2 Mechanically Induced Fracture Development and Response in Wellbore Systems

Fractures in wellbore cements are typically mechanically induced and usually caused by poor cementing, shrinkage, expansion/contraction, and thermal gradients. For instance, incomplete mud removal during cement placement results in voids and fractures within the cement sheath [Zhang and Bachu, 2011]. Cement shrinkage during curing can result in the development of a microannulus along steel-casing/cement interface, cement/formation interface, or fractures within the cement itself [Dusseault et al., 2000]. Differential expansion and contraction of the steel casing, cement sheath, and the surrounding formation from pressure and temperature gradients during operations has also been shown to produce microannuli between the steel-casing/cement or cement/formation contact [Lavrov et al., 2015].

Once formed, behavior of fractures within cement sheaths can be altered by changes in stress conditions. For instance, changes in stress on wellbore cements are induced by wellbore operation (pressure and temperature of fluid inside casing imposing stresses) [Wiprut and Zoback, 1999], deformation of adjacent formations [Sobolik and Ehgartner,

2006; Wiprut and Zoback 1999], or expansion/compaction of underlying reservoirs. Stress changes deform fractures and consequently can change the permeability of the fracture. Huerta et al (2011) split a cement core into two halves, mated them back together with a slight offset (1 mm) and placed the mated halves inside a pressure vessel. A hydrostatic confining stress from 1.4 MPa to 5.5 MPa was applied to the cement core. Permeability measurements (interpreted as a hydraulic aperture) were made using tap water at incremental levels of stress. To mitigate capture of significant chemical reactions between tap water and cement, permeability measurements were made during short timeframes at each stress level. Hydraulic aperture decreased from 25 μm at 1.4 MPa confining stress, to 11 μm at 5.5 MPa confining stress. Stormont et al (2015) measured the permeability (also interpreted as hydraulic aperture) of a fracture along the steel casing/ cement interface. At a confining stress of 4 MPa the hydraulic aperture was 100 microns, and when confining stress was increased to 21 MPa the hydraulic aperture was reduced to 47 microns.

During CO_2 injection, the thermal stresses, accompanied by injection and the improper centralizing of the casing, create, and can enlarge fractures in wellbore cement [Nygaard et al., 2014]. If injection of CO_2 follows a cyclic pattern, the stress cycling also enlarges the fracture's aperture [De Andrade et al., 2014].

Similar to the mechanism used for hydrofracturing of shale for resource recovery, fluid pressure within a cement fracture may cause vertical propagation [Carey et al., 2013] and

allows fluid migration to shallow strata or leakage to the surface/atmosphere [Dusseault et al., 2000].

1.3 Interfacial Reactivity of Water and Cement

1.3.1 Effect of Low Salinity Water Reactivity with Cement

The interaction between water and cement within a wellbore can cause reduction in the cement's permeability by chemical alteration of the cement. Loosveldt et al. (2002) injected water at a pressure of 1.5 MPa through an intact cement core. They found the cement's permeability decreased due to dissolution/precipitation of portlandite, swelling of calcium silica hydrate (C-S-H), hydration of non-reacted cement, and absorption of water [Loosveldt et al., 2002;]. Portlandite ($Ca(OH)_2$) and C-S-H ($CaSiO_2H_2O$) are two of the main calcium-containing solid phases in cement. Dissolution/precipitation has been found to clog pores and decrease porosity, which prevents penetration of fluid [Brunet et al., 2013].

In contrast, other studies show that dissolution of portlandite, or decalcification of C-S-H increases porosity of the matrix, and consequently increases permeability by forming enlarged pore networks. Jain and Neithalath (2009) immersed cement cubes in de-ionized water for a period of 90 days. Using thermo-gravimetric analysis (where physical and chemical changes are measured as a function of increasing temperature), changes in mass of the samples were compared to unreacted cement, and mass changes for both portlandite and C-S-H were measured and interpreted as a change in porosity. The results of the experiment indicated a porosity increase up to 11% for reacted samples. Marchand

et al (2000) compared nuclear magnetic resonance imaging (NMRI) results of unreacted cement to cement immersed in de-ionized water and used results to determine hydraulic diffusivity with numerical model software. This approach found that hydraulic diffusivity of the cement increases with increased leaching of portlandite. The numerical model revealed leaching 90 percent of calcium from portlandite can increase hydraulic diffusivity by a factor of 20 or more.

Carde and Francois (1999) evaluated mechanical effects of leaching calcium from cement phases by reacting cement with ammonium nitrate (NH_4NO_3) as a surrogate for de-ionized water. Solutions containing ammonium nitrate accelerate the same leaching processes as water by a factor of 300 [Carde et al., 1997]. Cement samples of different mix-designs (one mix-design replaced 30% of cement klinker with silica fume to inhibit "selective attack" of C-S-H) were immersed in a 50% ammonium nitrate solution. The varying mix designs aimed to decouple mechanical effects induced from either a decrease in portlandite (by dissolution), or a decrease in C-S-H (by decalcification). Dissolution of portlandite led to a strength loss of 70%, whereas decalcification of C-S-H resulted in a strength loss of 6%. This difference was attributed to dissolution of portlandite producing a macropore network and the decalcification of C-S-H producing a micropore network. Similarly, Agostini et al. (2007) submerged cement samples in an ammonium nitrate solution to leach calcium and decalcify of C-S-H for a 16 day period, and found that permeability increased two orders of magnitude, and an 85% loss in the cement's strength. Furthermore, Yurtdas et al. (2011) immersed cement in ammonium nitrate solution at 90° C, and measured a porosity increase ranging from 37 to 56% and a

decrease of 61 % in compressive strength. It was also found from the same study that cohesion within the cement matrix decreased 33%, and friction coefficient was reduced by 63%, the combination of which indicates plastic deformation would occur at lower stresses.

1.3.2 Effect of Brine Reactivity with Cement

Chemical composition of brines affects the reactivity with cement, and may have a direct impact on mechanical properties within the cement matrix. Duguid and Scherer (2010) found that a calcium-saturated brine does not degrade or decrease cement's mechanical properties. They injected water through a calcite chamber (ensuring saturation), then pumped water at 50°C and a pH of 5 into a vessel holding a cement sample. After 26 days of exposure, no degradation of the cement itself was observed. This finding was evident through inductively coupled plasma-optical emission spectroscopy (ICP-OES) data which showed similar concentrations of injected/effluent solution concentrations, and X-ray diffraction analysis of the cement showed identical peaks that exhibited no significant differences between a reacted and unreacted cement sample. These results imply that a water saturated with calcium prevents the dissolution of portlandite and decalcification of C-S-H that occurs with water that is not calcium saturated.

Acidic brines, however, such as those associated with CO_2 sequestration, induce reaction zones (Figure 1.1) in cement that alter its mechanical properties [Walsh et al., 2014; Huerta et al., 2012; Kutchko et al., 2007]. These reaction zones are commonly referred to

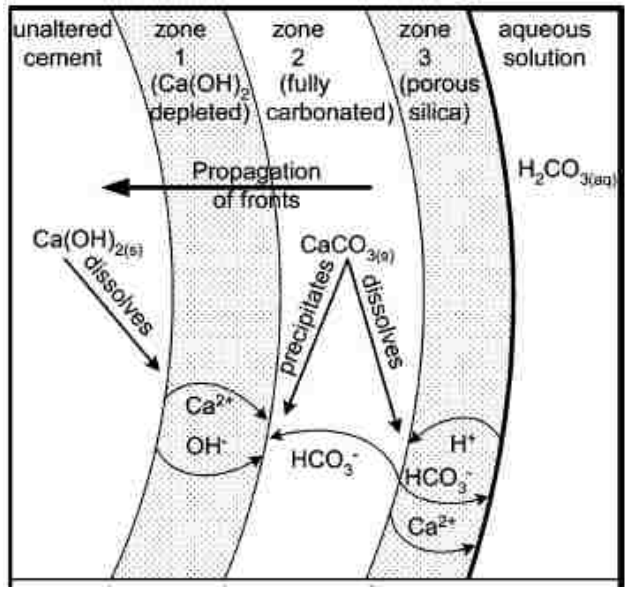

as: portlandite-depleted, fully carbonated zone, and a porous silica [Kutchko et al., 2007]. In an acidic brine environment, typical dissolution rates of portlandite occur up to four orders of magnitude faster than decalcification of C-S-H [Baur et al., 2004; Marty et al., 2009].The reaction fronts tend to produce a lower elastic modulus than unreacted cement, with the exception of the fully carbonated layer where stiffness and yield strength are found to be at least equal to unreacted cement [Walsh et al., 2014].

Kutchko et al (2007) saturated a cement sample with a 1% NaCl-CO_2-brine in a pressure vessel at 50°C and a pressure of 30.3 MPa. The brine's reactivity with cement caused dissolution of calcium-carbonate and led to C-S-H converting to amorphous silica gel and the decalcification of unhydrated cement. Hardness values were obtained on reacted and

unreacted samples by indenting the materials surface with a hard-tipped device with a prescribed force and the size of indentations correlate to particular hardness values; smaller indentations have larger hardness values. Hardness values in the reacted samples were less than 50% of those in the unreacted samples. This result was attributable to the presence of silica gel which lacks structure and an increased porosity as a consequence of decalcification. SEM imaging and EDS data were used qualitatively to observe changes in porosity by comparing altered zones where large pores developed to less altered zones and where pores were filled with calcite.

1.4 Effect of Brine Flow on Physical and Chemical Characteristics of Cement Fractures

Fluid flowing through cement fractures allows greater opportunity for reactions between cement and fluid to occur. The chemical reactions, in turn, affect the mechanical behavior of the fracture. Stress applied normal to a fracture that has been reacted with a CO_2 brine exhibits deformations that are irrecoverable [Huerta et al 2011]. Plastic behavior is attributed to initial plastic deformation of asperities and a decrease of mechanical properties in the cement due to alteration from acidic brine (e.g. elastic moduli and hardness). Measurements of hardness can be also used to determine the elastic modulus within an accuracy of 5% [Oliver and Pharr, 1992]. Decreases in hardness were a result of an increase in porosity from dissolution of portlandite and decalcification of C-S-H [Huerta et al, 2011; Mason et al., 2013]. Huerta et al. (2011) followed their measurements of flow through a cement fracture using tap water with measurements an acidic brine. Confining stress was cycled up to a maximum of 5.5 MPa and the permeability of the

fracture was interpreted as a hydraulic aperture both before reaction with brine (using tap water) and after. Before reaction, plastic deformation of asperities was indicated by the aperture decreasing from 25 μm at a normal stress equal to 1.4 MPa, to 11 μm at 5.5 MPa. A subsequent cycle exhibited an elastic response. After reaction, the same stress cycle was applied and the aperture's response was similar, but the values reduced by nearly 50%- indicating that acidic brine induces a self-healing effect [Huerta et al., 2012; Huerta et al., 2011]. The self-healing effect was attributed to mineral precipitation as the high pH of the pore fluid mixed with calcium-rich brine inducing precipitation. Huerta et al's (2011) study also found that the acidic brine flow was confined to distinct pathways as precipitation along the fracture resulted in preferential pathways.

Walsh et al (2014) injected an acidic brine (Equation 1) through fractured specimens comprised of artificially roughened/gridded cement mated against a caprock. They found that hydraulic apertures decreased up to 75% in core-flood tests due to dissolution of portlandite (Equation 2) and precipitation of calcite (Equation 3).

$$CO_{2(aq)} + H_2O \rightarrow H_2CO_{3(aq)} \qquad \text{(Equation 1)}$$

$$Ca(OH)_{2(s)} \rightarrow Ca^{2+}_{(aq)} + 2OH^-_{(aq)} \qquad \text{(Equation 2)}$$

$$Ca^{2+}_{(aq)} + HCO_3^-{}_{(aq)} + OH^-_{(aq)} \rightarrow CaCO_{3(s)} + H_2O \qquad \text{(Equation 3)}$$

The fracture was subjected to a normal stress of 3 MPa, and changes in fracture geometries were observed using X-ray tomography (XRTC) to quantify deformations of the surface. XRTC indicated plastic deformation occurring along the fracture. Deformations occurred where the alteration was physically apparent and yielded the lowest hardness values.

Abdoulghafour et al. (2013) injected CO_2-enriched brine at 2 ml/min at 60° C through a fractured cement which was subjected to normal stress of 10 MPa. Under these conditions a 42-μm wide fracture healed in a 24 hour period. This healing was attributed to decalcification of the C-S-H gel forming/swelling within the fracture. They questioned, however, how this "seal" would be sustained if flowrates were to increase and if the initial aperture was larger than tens of microns.

1.5 Effect of Brine on Carbon Steel Corrosion

Corrosion of steel casings in wellbores presents another challenge in understanding the impact brine has on fractured cement sheaths. Proper placement and coverage of cement is identified as the most important method to prevent steel casing corrosion [Choi et al., 2013]. Casing leakage, due to corrosion, can allow fluids to communicate from inside to outside the well, or vice-versa, and for oil and gas recovery creates a large financial impact [Brondel et al., 1994].

In a CO_2 brine environment, presence of alkaline materials (e.g. portland cement) can lead to bicarbonate contributing greatly to corrosion of the steel casing [Han et al., 2011]. Alkalines are also used to adsorb CO_2 for capture, and the resulting fluid, which is transferred through steel casing to underground reservoir, contains bicarbonate as a predominant species which can induce corrosion [Zhang and Martin, 2011].

Carbon steel exposed to brines with increased salt concentration accelerates corrosion, and has exhibited corrosion rates of several millimeters per year [Han et al., 2011]. The comparison of different salt concentrations impact on corrosion rates was investigated using reacting solution with 1% and 10% concentrations of NaCl; both of which had pH values ranging from 4-8. It was revealed that at lower pH values (pH=4) the 1% concentration solution had an increased corrosion rate of 3.2 mm/year, where 10% was 2.3 mm/year. This was attributed to lower CO_2 solubility at higher salt concentrations, therefore lower carbonic acid yielded decreased corrosion rates. In contrast, with a pH of 8 the 1% solution had a rate of 2.9 mm/year, and 10% was 3.9 mm/year. This change was due to increased salt concentrations which resulted in greater bicarbonate concentrations and consequently greater corrosion rates.

1.6 Knowledge Gaps

A more complete understanding of coupled physical-chemical mechanisms that contribute to the opening or closing of fractures is necessary to quantify risks associated with wellbores used for a variety of applications [Carroll et al., 2016]. Physical-chemical impacts to fractured cement due to reaction with acidic brines have been the most common area of research. To date, most research indicates that dissolution of CO_2 into brine lowers the pH, is able to dissolve calcium-containing cement phases, and contribute to either a self-healing effect or reduced permeability of fracture by precipitation of calcite and presence of stress normal to fracture. In contrast, there is a comparatively much less knowledge of the physical and chemical alterations that may occur in cement fractures from saline brines, such as those that may be associated with hydrofracture flowback waters [Haluszczak et al., 2013].

1.7 Research Objective

The principal objective of this study is to determine the chemical reactivity and behavioral changes fractured wellbore cement undergoes when subject to confining stress and reacted with de-ionized water or brine that is exposed to carbon steel. In order to determine the changes from such interactions, flow measurements were made on a fractured cement core using nitrogen gas (serving as a baseline), de-ionized water, and brine under a range of applied confining stresses and fluid pressures to calculate the permeability of the fracture. Changes in permeability (interpreted as hydraulic aperture) due to stress changes or alteration of fracture surface were measured to identify the physical impacts of a non-acidic that can be couple with chemical changes.

Comparing measurements of hardness and images of fracture surfaces among unreacted, de-ionized water reacted, and brine reacted cements indicates if alteration along the fracture surface has taken place. A decreased hardness in reacted cement fracture surfaces, compared to unreacted, suggests chemical alteration of the cement has changed its mechanical behavior. Imaging the fracture surfaces provides evidence of alterations that have occurred.

Chemical changes along the fracture surface were examined through compositional analyses of fracture surface, injected fluids, and effluent fluids. Changes to the calcium concentrations in fluids and calcium-containing phases in cement (e.g. portlandite) complement the observed mechanical response. If portlandite decreases then hardness is

expected to decrease. Change in portlandite content of cement is expected to influence calcium concentrations in fluids flowing through cement.

Figure 1.2 represents the anticipated reactions between cement and non-acidic brine that will lead to dissolution of portlandite (Equation 4), precipitation of calcite (Equation 5), decreased hardness of cement fracture surface, and decreased permeability of the fracture.

$$Ca(OH)_{2(s)} + H_2O_{(aq)} \rightarrow Ca^{2+}{}_{(aq)} + H_2O_{(aq)} \qquad \text{(Equation 4)}$$

$$Ca^{2+}{}_{(aq)} + OH^{-}{}_{(aq)} + HCO^{3}{}_{(aq)} \rightarrow CaCO_{3(s)} + H_2O_{(aq)} \qquad \text{(Equation 5)}$$

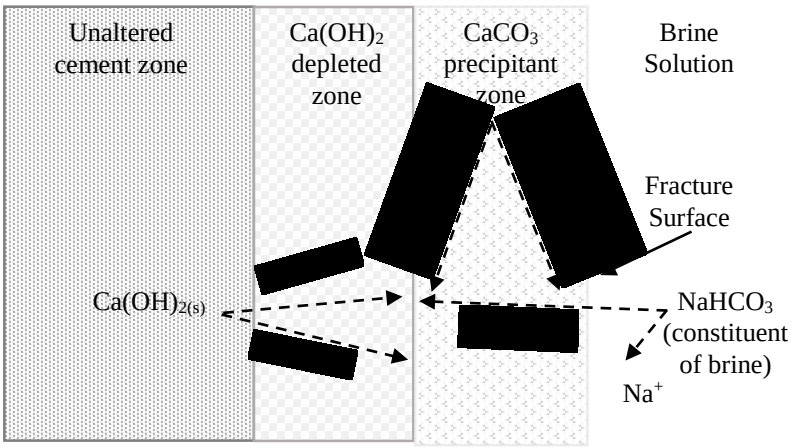

Figure 1.2 Reactions between cement's portlandite and non-acidic brine that leads to a zone of decreased portlandite and a zone of calcite precipitation.

Coupling the physical-chemical impacts a non-acidic brine, or water, imposes on cement fractures advances our understanding of wellbore behavior in the various environments a wellbore is expected to survive.

Chapter 2

Materials and Methods

2.1 Sample Preparation

Three cylindrical cement cores with a diameter of 102 mm and a length of 180 mm were cast using a ratio of 1000 g Type I cement, 330 g water, 100 g silica fume, and a 7 g plasticizer. The three samples (referred to throughout as unreacted, de-ionized reacted (DI), and brine reacted (BR)) were cured in a humid environment at 50 °C for a minimum of 21 days. A fracture in each sample created two halves which were nearly equal in size and was developed through tensile-splitting in a Brazilian test configuration. For samples DI and BR, a 0.6 mm thick perforated carbon steel sheet was placed on opposing and opposite ends of the cement core halves to offset the fracture surface, so the fracture did not perfectly mate when subjected to confinement (Figure 2.1). The carbon steel sheet allowed for reaction with fluid that was injected through the fracture. These cores were then wrapped with a thin plastic film to allow ease of install/removal from the pressure vessel (Figure 2.1).

The unreacted sample was used as a baseline for determining changes in mechanical property, hardness, and chemical composition of the two reacted cements.

The DI sample is reacted with de-ionized water in a flow test. After the flow test hardness are measured, and compositional analyses are performed to identify differences in the

results obtained from the unreacted cement, and BR. Testing sequence performed on BR sample is described in Section 2.2.1.

Figure 2.1. Fractured cement core with perforated sheets attached and wrapped with a release film

DI and BR were placed in a pressure vessel that was used to apply a constant hydrostatic confining stress up to 16.5 MPa (all confining stresses are hydrostatic) and allowed fluid injection and collection (Figure 2.2). Tests were conducted on the BR sample using nitrogen gas, de-ionized water, and a brine. Nitrogen gas served as a non-reactive fluid that allowed measurements to be made at different stages of the testing sequence and served as a baseline for comparison; confirming results found from water and brine testing. De-ionized water was obtained from an 18 mega-ohm ultra-pure water dispenser. Brine composition (per 1L of water: calcium chloride ($CaCl_2$)-36.75 g, sodium chloride (NaCl)- 117.29 g, sodium bicarbonate ($NaHCO_3$)- 0.09 g) was modeled after saline flowback waters sampled from wells in an experiment conducted with Marcellus Shale [Haluszczak et al 2013].

Only one flow test using de-ionized water, with a confining stress of 11.1 MPa, was performed on the sample DI. This single test was used to measure the hardness of the cement's fracture surface after it has reacted with only de-ionized water.

2.2 Equipment and Methods for Mechanical Experiments

For gas flow tests, nitrogen gas cylinders were used to supply the upstream side of the sample. The upstream gas pressure was controlled and measured with a regulator in series with a digital pressure gage. The downstream pressure could be controlled with a needle valve to regulate flow and measured with a pressure gage; in the tests reported here, the downstream outlet pressure was atmospheric. Volumetric gas flow was measured with a rotameter in which interchangeable flow tubes could accommodate flows ranging from 0 to 60,000 cc/min.

Testing with liquids were conducted using a piston pump that supplied water and brine to the upstream side of the sample at flow rates that ranged from 0.01 mL/min to 10 mL/min. The upstream pressure was measured with a digital pressure gage. The downstream was directed to a collection reservoir at atmospheric pressure.

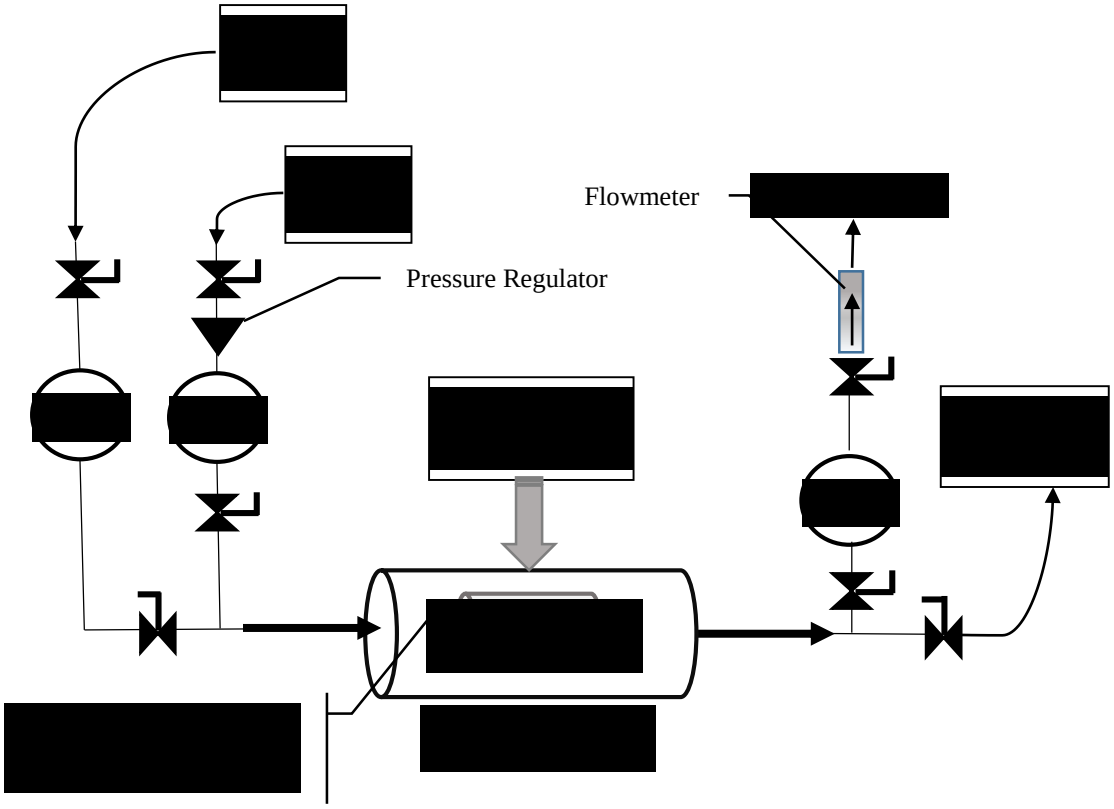

Figure 2.2 Schematic of test configuration for flow tests. Circles with "$P_{gas/liquid}$" are pressure gauges.

The differential pressure between upstream/downstream, along with flowrate, was used to determine the permeability of the cement fracture and was interpreted as an equivalent hydraulic aperture. The amount of flow through the sample correlated with a permeability that was always more than an order of magnitude greater than the flow attributable to cement. The hydraulic aperture (b) [Witherspoon et al., 1980] is:

$$b = \left[\frac{12\mu l q}{w\gamma\Delta h}\right]^{1/3} \qquad \text{[Equation 6]}$$

In Equation 6 μ is fluid viscosity, *l*- sample length, q- flux through fracture, w- width of fracture, γ- specific weight of fluid, and Δp- difference in fluid pressure across sample. Reynold's numbers were calculated for all flow tests, and were found to be below the value of 10 where laminar flow transforms to turbulent [Hassanizadeh and Gray, 1987; Huitt, 1956].

2.2.1 Test Sequencing for Stress Cycles to a Fractured Cement

Hydraulic aperture (an interpretation of permeability) of sample BR was measured using the following sequence described in Table 2.1.

Table 2.1 Testing sequence, conditions, and information to be obtained. Note: between each "Test Run" the confining stress on the sample was unloaded and reloaded.

Test Run	**Conditions**	**Information to be obtained**
Nitrogen gas tests with varying confinement	1st Confining stress sequence- 5.5 MPa, incrementally increased to 16.5 MPa, incrementally reduced to 5.5 MPa 2nd Confining stress sequence- 4.1 MPa, , incrementally increased to 16.5 MPa, incrementally reduced to 4.1 MPa	Initial change in hydraulic aperture in response to confining stress with an inert fluid and subsequent response to repeated conditions of confining stress.
De-ionized water tests with varying confinement pH- 7.47	Confining stress sequence- 4.1 MPa, , incrementally increased to 16.5 MPa, incrementally reduced to 4.1 MPa	Change in hydraulic aperture in response to varying confining stress Compare to behavior of nitrogen gas tests

De-ionized Water Flow Test pH- 7.47	Sustained confining stress of 11 MPa Volumetric flowrate ranged from 2-10 mL/min (adjustments made to remain in allowable range of upstream pressure gauges)	Change in hydraulic aperture. Change in chemical composition of the effluent.
2nd Post-water nitrogen gas tests	Confining stress sequence- 4.1 MPa, , incrementally increased to 16.5 MPa, incrementally reduced to 4.1 MPa	Determine hydraulic apertures in response to confining stress.
Brine Flow Test pH- 6.18	Sustained confining stress of 11 MPa Volumetric flowrate ranged from 0.25-2 mL/min (adjusted to remain in allowable range of upstream pressure gauges)	Change in hydraulic aperture. Change in chemical composition of the effluent.
Post-brine gas tests	Confining stress sequence- 4.1 MPa, , incrementally increased to 16.5 MPa, incrementally reduced to 4.1 MPa	Determine hydraulic apertures in response to confinement.

2.3 Post Test

2.3.1 Chemical Analyses for Solids (Cement) & Liquids (Fracture Fluid)

To identify correlations between the mechanical response and chemical alteration of the fracture surfaces, effluent samples and fragments of cement (both reacted and unreacted) were collected for analysis. Solid phase analyses that were performed on the cement's fractured surfaces consisted of X-ray diffraction (XRD, Rigaku SmatLab using Cu K-alpha radiation and a D/teX 1 dimensional detector with a Ni K beta filter), and scanning

electron microscopy (SEM, FEI Quanta 3d FEG)/ energy dispersive X-ray spectroscopy (EDX, Oxford Instruments INCA). Portions of the reacted cements were broken off and acidified for solution phase analysis as well. Acidified cement fragments were filtered through 0.45 μm membranes. For solution phase analysis a Perkin-Elmer Optima 5300 DV Inductively Coupled Plasma-Optical Emission Spectrometer (ICP- OES) and a Perkin-Elmer Nexion 300D inductively coupled plasma-mass spectrometer (ICP-MS) system were used to analyze the metal concentration in liquid samples.

2.3.2 Hardness Measurements of Reacted and Unreacted Fracture Surfaces

The hardness of the cement along the fracture(s) are evaluated using micro-hardness values with a Vickers 402 MVD imposing a 300 gram force. Changes in hardness along fracture interfaces are examined to evaluate where alterations are evident as a result of fractures being exposed to de-ionized water and brine. Hardness values (HV) are compared to those gathered from an unreacted cement fracture. Three different cement cores are evaluated: unreacted, DI, and BR. For reacted samples two ranges of values are introduced: *soft*- HV<75, *hard*- HV>75.

Since the surfaces could not be polished, as this would remove the constituents that may have altered behavior, care was taken to ensure that indentations were in the flattest of regions for the most accurate values possible. Several hardness values are collected for the unreacted sample at arbitrary locations to mitigate measuring heterogeneities along the fracture.

Chapter 3

Results and Discussion

3.1 Initial Mechanical Response of Fractured Cement Cyclic Loading

Initial nitrogen gas testing of BR identifies a plastic response induced by a normal stress applied to the cement fracture. Confining stress was cycled from 5.5 MPa, increased incrementally to a maximum confinement of 16.5 MPa, and finally decreased incrementally to 5.5 MPa (Figure 3.1a). The hydraulic aperture at 5.5 MPa was 59 μm. When a maximum confinement of 16.5 MPa was applied, the hydraulic aperture decreased to 35 μm (~40% reduction). Decreasing confining stress to 5.5 MPa increased hydraulic aperture to 39 μm. The initial decrease in hydraulic aperture is largely due to "strain hardening" of asperities, consistent with the results of Huerta et al. (2011).

After strain hardening occurs, an elastic response can be observed when a subsequent cyclic load was applied to the fracture. Beginning with 4.1 MPa, incrementally increasing to 16.5 MPa, and lastly down to 4.1 MPa yields hydraulic apertures of 41, 31, and 38 μm respectively (Figure 3.1a). This response was also comparable to the results of Huerta et al's 2011 study which identifies an elastic response on the second cyclic loading in which tap water was used as a non-reacting fluid.

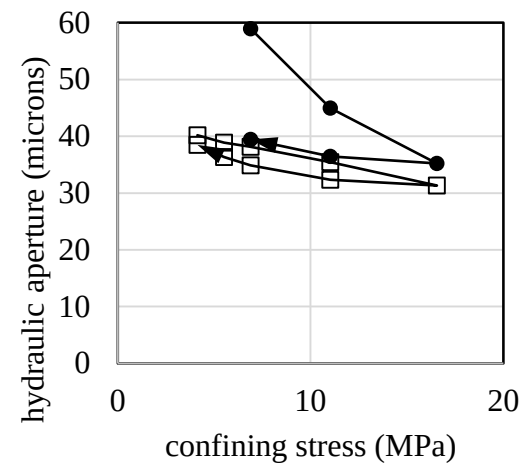

a)

nitrogen gas 1st cycle

nitrogen gas 2nd cycle

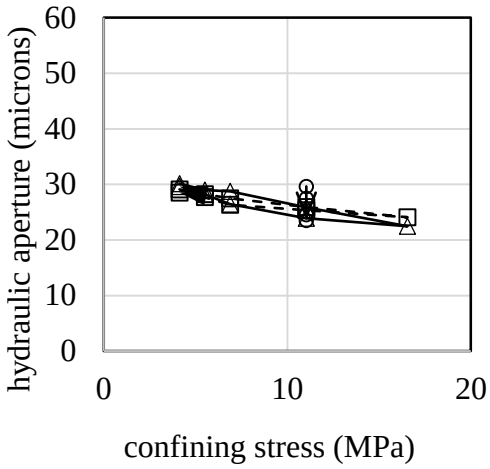

b)

de-ionized water cycle

post-water gas cycle

de-ionized flow test

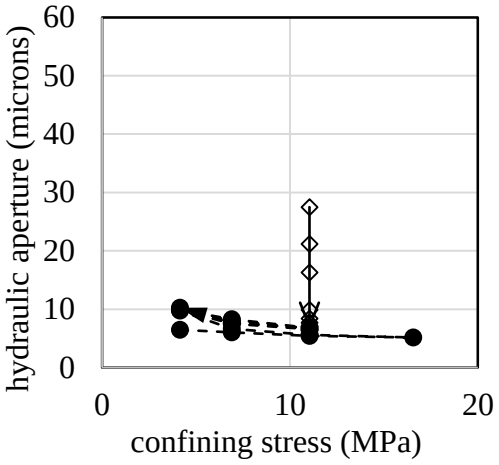

c)

post-brine gas cycle

brine flow test

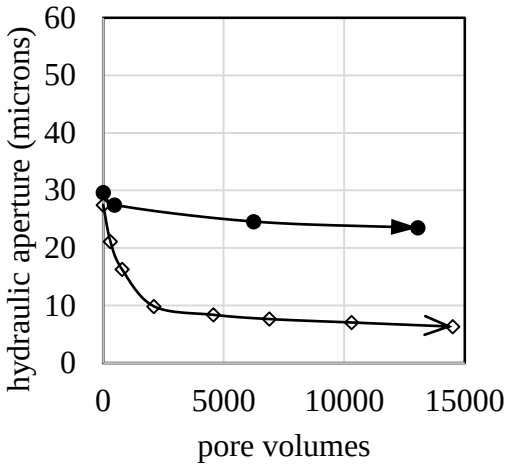

d)

de-ionized flow test

brine flow test

3.2 Mechanical Response of Fractured Cement Reacted with De-ionized Water

The fracture's response of BR to a repeated normal stress cycle reacted with de-ionized water suggests that the hydraulic aperture consistently decreased. Like previous confinement cycles, stresses of 4.1 MPa-16.5 MPa-4.1 MPa were applied, which yielded hydraulic apertures of 30, 22, and 30 μm respectively. These values of hydraulic aperture indicate an elastic response, however, they are roughly 25% smaller than results from the last nitrogen gas test (Figure 3.1b).

Following the cyclic loading described above, attempts were made to measure permeability as a function of pore pressure within the fracture. These tests produced inconsistent results and were not pursued further. Following these efforts a longer-term flow test was then performed with a constant confining stress.

Hydraulic apertures were measured over time (interpreted as pore volumes) while confining stress was sustained at 11 MPa. Initial aperture for the flow test was 30 μm which indicates the aperture actually increased from the previous measurement. This increase is believed to be either from removal of precipitants along fracture surface, or shear movement when efforts to test pore pressure effects were attempted. After injecting approximately 13,000 pore volumes of de-ionized water, the hydraulic aperture was found to be 24 μm (Figure 3.1b).

To evaluate whether the decrease seen in water results compared to gas was not just an artifact of using different fluids, hydraulic apertures were determined using nitrogen gas.

This sequencing provides a comparison of fracture response for unreacted and reacted (before water interaction and after water interaction). Fluid within the fracture was blown out using shop air at 0.7 MPa, followed with flow measurements for identical cyclic loading of 4.1 MPa-16.5 MPa-4.1 MPa. This cycle yielded apertures: 29 μm, 24 μm, and 28.5 μm respectively (Figure 3.1b). These values were close to the results for de-ionized water and lower than previous gas results indicating that some alteration(s) has taken place allowing a decrease in hydraulic aperture.

3.3 Mechanical Response of Fractured Cement Reacted with Brine

Mechanical results suggest that flow of brine through a cement fracture causes a reduction in aperture. Introduction of brine to the fracture was in the form of a flow test. Similar to the de-ionized water flow test confinement was sustained at 11 MPa. At the time of initial injection the hydraulic aperture was 28 μm, and decreased substantially to 10 μm (~65% reduction) after just 2000 pore volumes of brine was injected. Ultimately the aperture decreased to 6 μm (aperture for an intact cement core was calculated and has an equivalent hydraulic aperture of about 2 μm) after 14,500 pore volumes of brine had been injected- a total reduction of about 80% (Figure 3.1d). The concluding aperture of 6 μm is comparable to the study of Huerta et al. (2011) who found that alterations from acidic brine reduced a fractured cement's aperture to about 7 μm. The hydraulic aperture's response to brine flow and its sustained confinement indicate that brine's reactivity with cement contributes largely to the fracture's self-healing behavior.

A post-brine nitrogen gas test confirms the hydraulic aperture had decreased due to reactivity with brine. The cyclic loading of 4.1 MPa-16.5 MPa-4.1 MPa yield similar values of that at the end of the brine flow test; 6.5, 5, 10 μm respectively (Figure 3.1c).

3.4 Surface Hardness Comparison for Unreacted, De-ionized Reacted, and Brine Reacted Fractured Cement

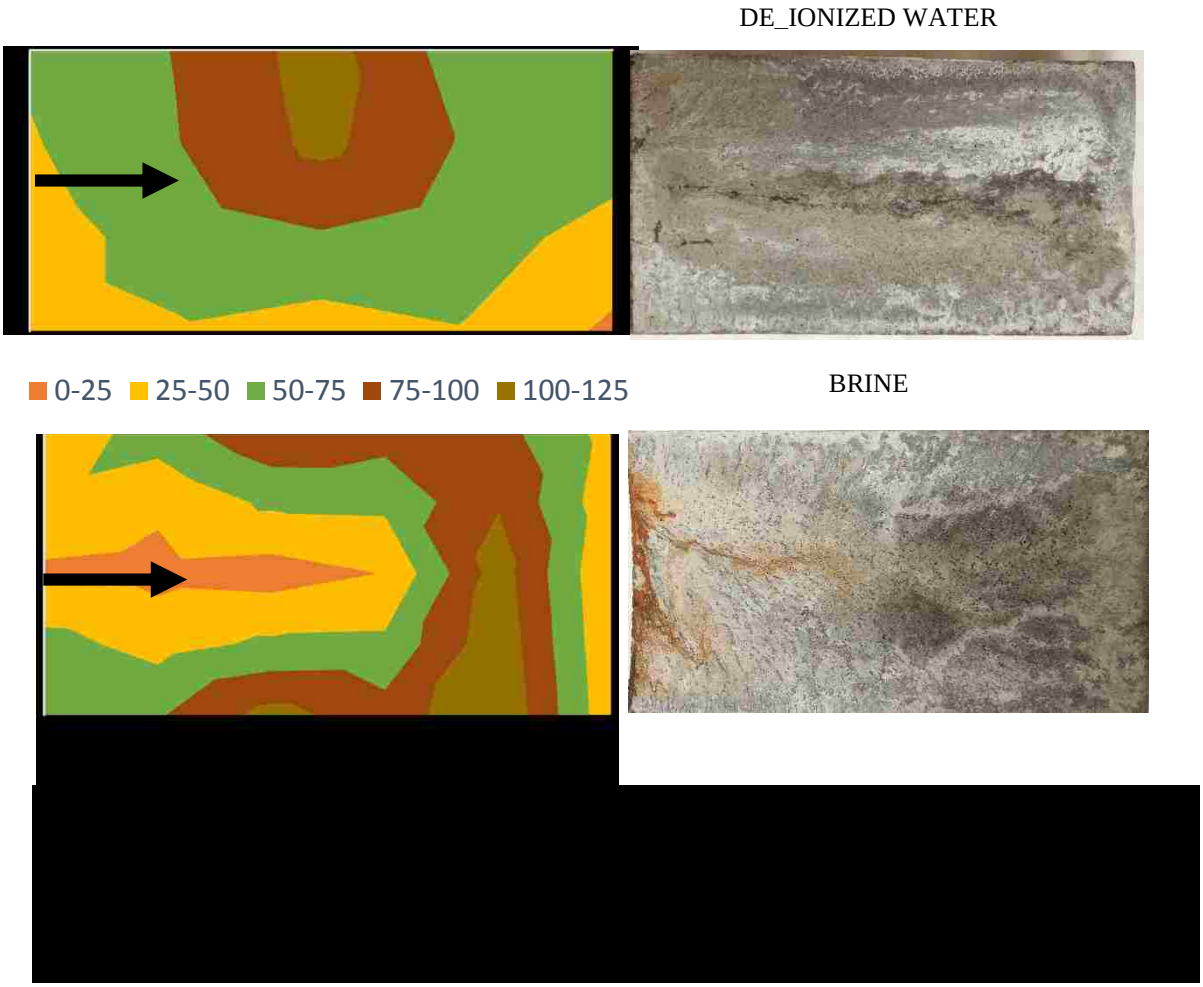

Measurement of hardness values (HV) along the fracture surfaces identify where mechanical properties (hardness and elastic modulus) of the cement changed due to

cement reacting with de-ionized water and brine due to the change in chemical composition along the surface. HV for an unreacted cement fracture were taken at several points and yielded the following Vickers numbers: 283.3, 309.5, 279.2, 202.9, 168.3, and 201.1. These values have a mean of 241 and a standard deviation of 57. Reacted samples had hardness values that fell below this average, and in so-called '*soft'* regions, hardness values were significantly lower - up to an order of magnitude in some spots (Figure 3.7). These low values suggest that the cement's mechanical integrity have been reduced by alteration. The highest values of hardness on reacted cements were in the range for calcite found in Taylor's study (1949).

3.5 Interfacial Reactivity of De-ionized Water on Fractured Cement

Flow of de-ionized water through fractured cement caused a decrease in hardness and hydraulic aperture. To better understand the interaction between mechanical and chemical processes, further analyses were performed on samples of injected fluids, effluents, and both unreacted and reacted cements by using aqueous chemistry, microscopy, and diffraction.

ICP-OES analysis identified calcium being leached from the cement. Compositional change of injected fluid (de-ionized water) and effluent samples taken throughout the flow test were evaluated to determine change in calcium. Calcium's importance is rooted in its prominent role in dissolution/precipitation/decalcification among the two main calcium-containing phases of cement - portlandite and C-S-H. Initial calcium concentration for the effluent was 50mg/L and increased to nearly 140 mg/L after injecting 500 pore volumes and ultimately decreased to 70 mg/L at the end of injecting

13,000 pore volumes (Figure 3.3). The decrease seen in calcium concentration of the effluent is attributed to significant reduction in porosity from calcite precipitation which clogs pores and prevents further acid penetration [Brunet et al., 2013].

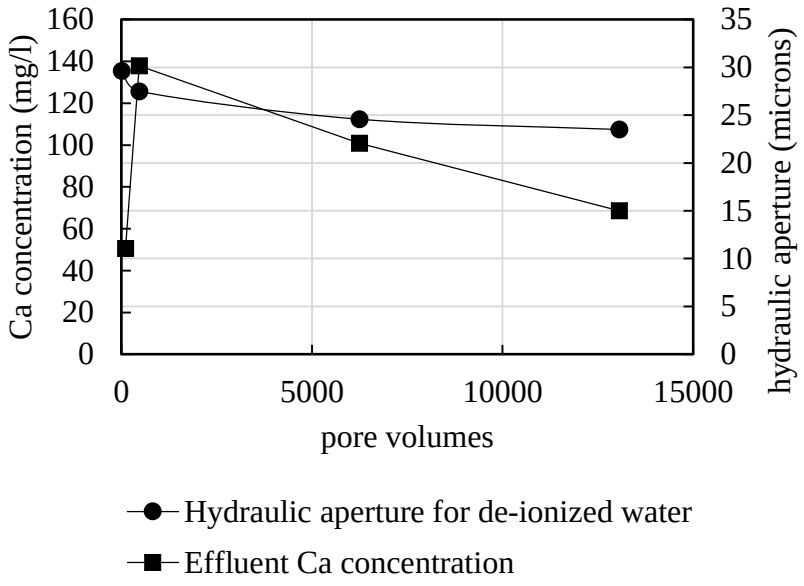

Figure 3.3 Calcium concentration of effluent and hydraulic aperture response under sustained confining stress of 11 MPa versus injected pore volumes of de-ionized water.

The presence of calcium in the effluent suggests that either dissolution of portlandite or decalcification of C-S-H occur during the duration of the experiment. Analyses of SEM images, EDX spectra, and XRD data of unreacted cement and cement reacted with de-ionized water were performed to evaluate specific chemical mechanisms. Compared to the physical appearance of unreacted fracture surface (Figure 3.4), DI's fracture surface (Figure 3.5 and Figure 3.6) displays a different shape. Small crystals forming were observed in the SEM image of the *hard* portion of the sample where silica and calcium are the predominant species determined in the EDX spectra (Figure 3.5). However in the *soft* regions of the sample these same crystal structures were not present and the shape

resembles unreacted cement, but with smaller sized crystals that appear to stack/layer (Figure 3.6). In the corresponding EDX spectra for *soft* there is mostly calcium and nearly negligible silica.

Calcium dissolving into the de-ionized water can remain in solution or precipitate as calcite along the fracture. XRD analysis for unreacted cement (Table 3.1) and cement reacted with de-ionized water indicate a 50% decrease in portlandite in the *soft* regions (likely caused by dissolution) while calcite increased 50% (caused by precipitation). The decrease in portlandite corresponding to a reduced hardness of the *soft, however*, is similar to the findings of Kutchko et al.(2007) where decreased hardness was measured in portlandite-depleted zones. There was no significant change in the C-S-H (Table 3.1-amorphous). Comparison between the unreacted and *hard* regions were relatively unchanged in both portlandite and calcite implying no significant alteration took place in these regions.

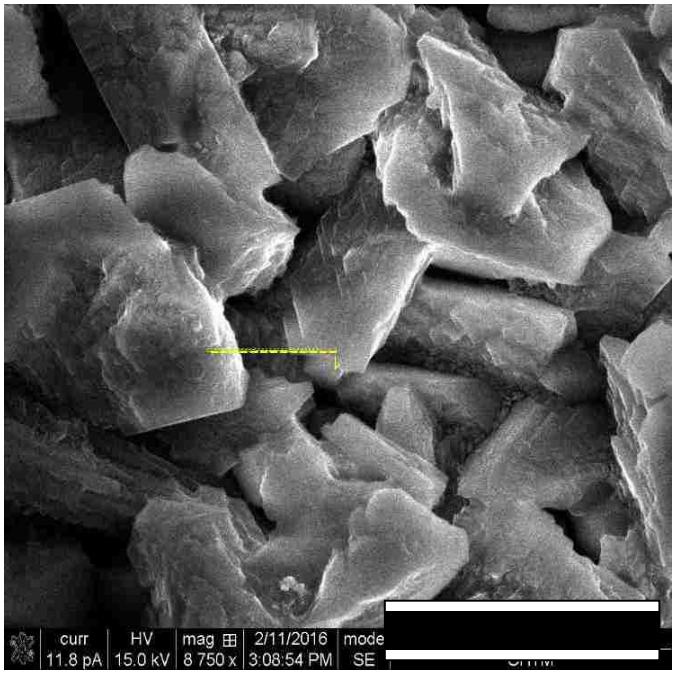
curr
11.8 pA
HV
15.0 kV
mag
8 750 x
2/11/2016
3:08:54 PM
mode
SE

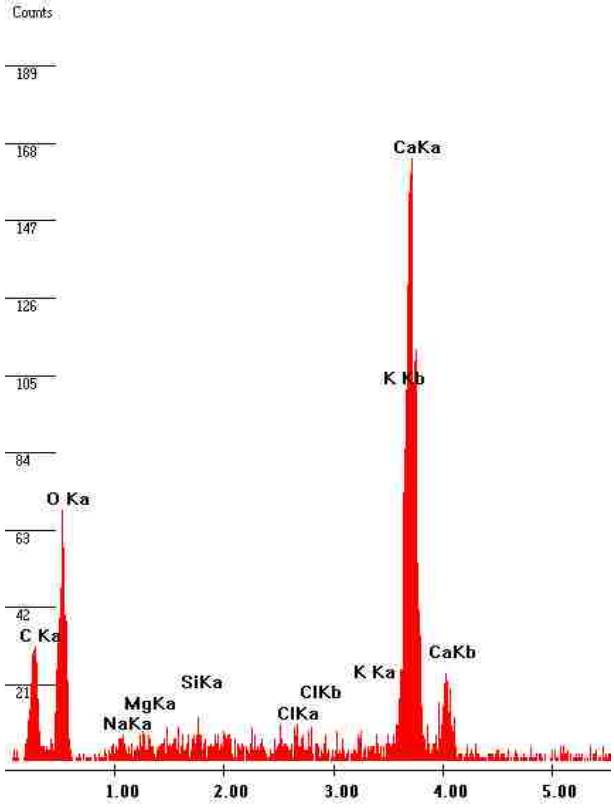
Counts
189
168
147
126
105
84
63
42
21
CaKa
K Kb
O Ka
C Ka
CaKb
K Ka
SiKa
ClKb
MgKa
ClKa
NaKa
1.00
2.00
3.00
4.00
5.00

[redacted]

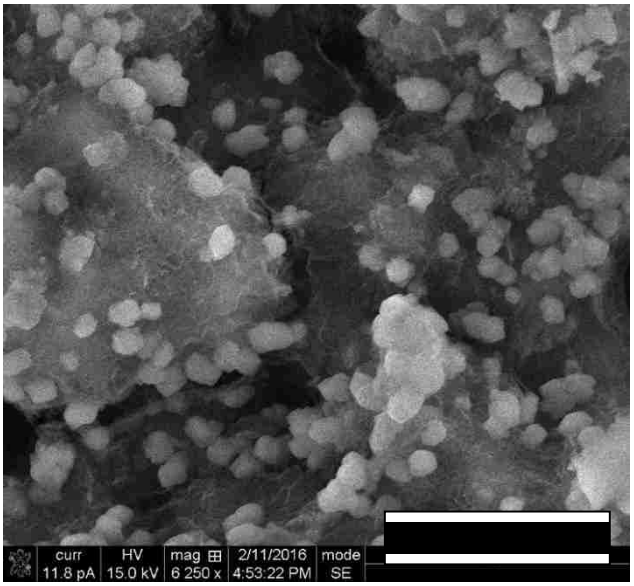
curr
11.8 pA
HV
15.0 kV
mag
6 250 x
2/11/2016
4:53:22 PM
mode
SE

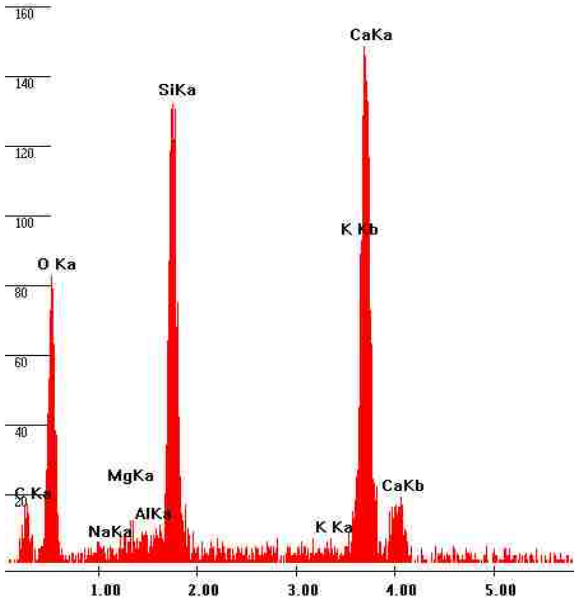
160
140
120
100
80
60
40
20
CaKa
SiKa
K Kb
O Ka
MgKa
CaKb
C Ka
AlKa
NaKa
K Ka
1.00
2.00
3.00
4.00
5.00

[redacted]

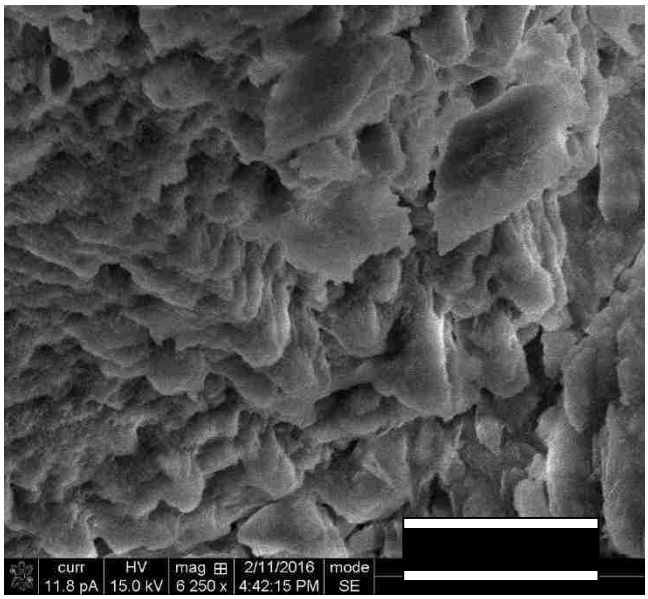
curr
11.8 pA
HV
15.0 kV
mag
6 250 x
2/11/2016
4:42:15 PM
mode
SE

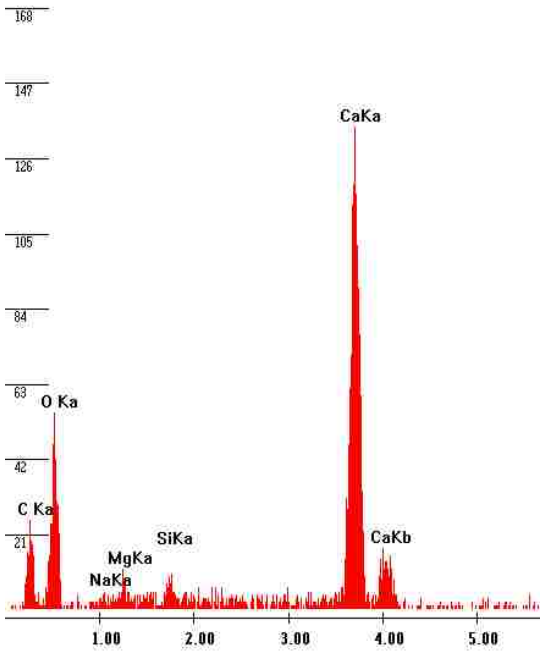
168
147
126
105
84
63
42
21
O Ka
C Ka
MgKa
SiKa
NaKa
CaKa
CaKb
1.00
2.00
3.00
4.00
5.00

[redacted]

Table 3.1 XRD analysis data for unreacted and de-ionized reacted cement. Quantity in parenthesis is estimated standard deviation (esd).

	Unreacted		DI Hard		DI Soft	
Phase Id	**Wt.% (esd)**	**Volume % (esd)**	**Wt.% (esd)**	**Volume % (esd)**	**Wt.% (esd)**	**Volume % (esd)**
Portlandite $Ca(OH)_2$	9.7 (0.3)	11.4 (0.3)	10.4 (0.3)	12.4 (0.4)	4.6 (0.2)	5.5 (0.3)
Hatrurite Ca_3SiO_6	14.9 (0.6)	12.3 (0.5)	13.8 (0.6)	11.5 (0.5)	14.1 (0.6)	11.9 (0.5)
Calcite $CaCO_3$	10.9 (0.4)	10.6 (0.4)	10.7 (0.4)	10.5 (0.4)	14.3 (0.4)	14.2 (0.4)
Monticellite $CaMgSiO_4$	2.7 (0.4)	2.3 (0.3)	3.6 (0.5)	3.1 (0.4)	3.2 (0.4)	2.7 (0.4)
$CaAl_4Si_2O_{11}$	0.8 (0.1)	0.6 (0.1)	0.9 (0.1)	0.6 (0.1)	0.7 (0.1)	0.5 (0.1)
Periclase, syn MgO	1.0 (0.2)	0.7 (0.1)	1.4 (0.2)	1.1 (0.1)	1.7 (0.2)	1.3 (0.1)
Brownmillerite Ca_2FeAlO_5	4.0 (0.1)	2.8 (0.1)	6.7 (0.4)	4.8 (0.3)	7.5 (0.4)	5.4 (0.3)
Amorphous + Others	56.0 (0.6)	60	52.4 (0.6)	59.5	54.0 (0.6)	58.5

Walsh et al. (2014) determined where material properties (e.g. strength, hardness, elastic moduli) had changed correlated to alterations in the cement's composition (Figure 1.1). Where portlandite or C-S-H was reduced, a corresponding reduction in mechanical properties occurred. Correlations between the decrease in hardness values of reacted cement and those of the unreacted, as well as change in the cement's chemical composition, suggest that material properties reduce where either portlandite or C-S-H decrease. In this study, the *soft* region's largest decrease in portlandite, corresponds to the largest decrease of hardness.

Decreasing calcium concentration in the effluent indicates a decreased interaction between water and cement. Decreased interaction between water and cement (e.g. reducing the amount of calcium leaching from portlandite) and the stabilizing hydraulic aperture determined in flow test results suggest that aperture reduction slows down as less calcium is leached. The decrease in calcium leaching may be a result of decreased permeability in the cement matrix (not the fracture) from dissolution/precipitation reactions similar to the findings of Loosveldt et al., 2002, or calcite precipitants causing porosity reduction which would clog pores and prevent penetration of fluids [Brunet et al., 2013].

No significant signs of corrosion were observed on the perforated steel sheet that was exposed to the injected water when conducting the flow test on DI, and none of the chemical analyses indicated presence of carbon steel constituents. This suggests that de-ionized water exposed to steel casing should not have any additional impacts on the fracture's behavior.

3.6 Interfacial Reactivity of Brine Flow on Fractured Cement

Flow of brine through a fractured cement causes a self-healing effect. When BR was removed from a pressure vessel, force had to be applied to split the fractured cement apart. For Sample DI, the two halves fell apart upon removal. Calcium concentration was slightly above 6000 mg/l in the first effluent sample retrieved and was approximately 65 % of injected concentration (9000 mg/l). At approximately 2000 pore volumes the effluent became comparable to the injection concentration and stabilized at that value thereafter (Figure 3.7). In the flow test and under sustained confinement, the first 2000

pore volumes of injection yielded a hydraulic aperture decrease from 28 μm to 10 μm. This decrease in hydraulic aperture and initial drop in calcium concentration in effluent suggests that calcium precipitates out of the solution along the fracture. The decrease of hydraulic aperture may also be the precipitant development leading to the forming of preferential pathways. After the first significant decrease in hydraulic aperture, continued injection of brine corresponded to a gradual decrease to 6 μm.

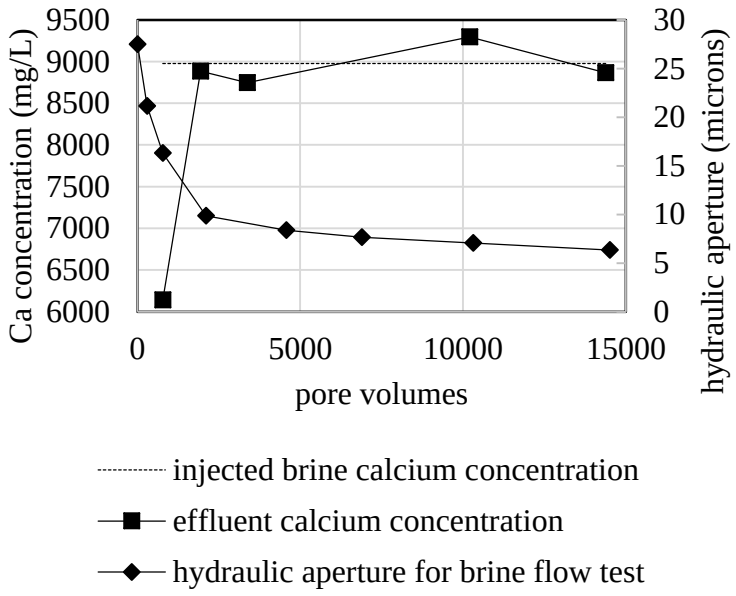

Figure 3.7 Calcium concentration of effluent and hydraulic aperture response under sustained confining stress of 11 MPa versus injected pore volumes of brine.

Calcium concentration in the effluent stabilized (the effluent concentration is approximately equal to the injected concentration) after approximately 2000 pore volumes. However the hydraulic aperture after injecting 2,000 pore volumes decreases from 10 μm to 6 μm at nearly 15,000 pore volumes. During this period it is not evident whether precipitation is causing the decrease in aperture or if the cement's composition and mechanical properties are allowing the fracture to become more compressible. As

with the flow of de-ionized water SEM imaging, EDX spectra, and XRD analysis were considered.

Table 3.2 XRD data for unreacted and brine reacted cements. Quantity in parenthesis is estimated standard deviation

	Unreacted		BR Hard		BR Soft	
Phase Id	**Wt.% (esd)**	**Volume % (esd)**	**Wt.% (esd)**	**Volume % (esd)**	**Wt.% (esd)**	**Volume % (esd)**
Portlandite $Ca(OH)_2$	9.7 (0.3)	11.4 (0.3)	4.1 (0.2)	4.9 (0.2)	0.5 (0.0)	0.6 (0.0)
Hatrurite Ca_3SiO_6	14.9 (0.6)	12.3 (0.5)	10.1 (0.6)	8.5 (0.5)	7.9 (0.6)	6.6 (0.5)
Calcite $CaCO_3$	10.9 (0.4)	10.6 (0.4)	27.8 (0.5)	27.4 (0.6)	24.8 (0.7)	24.3 (0.7)
Monticellite $CaMgSiO_4$	2.7 (0.4)	2.3 (0.3)	5.5 (0.5)	4.7 (0.4)	4.4 (0.5)	3.7 (0.4)
$CaAl_4Si_2O_{11}$	0.8 (0.1)	0.6 (0.1)	0.7 (0.1)	0.5 (0.1)	0.6 (0.1)	0.4 (0.1)
Periclase, syn MgO	1.0 (0.2)	0.7 (0.1)	0.4 (0.1)	0.3 (0.0)	0.8 (0.2)	0.6 (0.1)
Brownmillerite ● Ca_2FeAlO_5	4.0 (0.1)	2.8 (0.1)	3.9 (0.4)	2.8 (0.3)	3.9 (0.4)	2.8 (0.3)
Amorphous + Others	56.0 (0.6)	60	47.5 (0.6)	50.9	57.1 (0.7)	61

XRD analysis shows the reactivity of saline brine with cement has produced substantial changes in both portlandite and calcite contents. Calcite content of BR increased significantly compared to the unreacted - approximately 150 % for both *hard* and *soft* regions. Also, portlandite decreased about 50 % in the *hard* regions, and is nearly absent among *soft* regions (Table 3.2). Decrease of portlandite would reduce mechanical properties of the cement [Kutchko et al., 2007; Walsh et al., 2014]. As seen in Figure 3.2, hardness values are found to be well below the range for calcite - 105-145 for a 50 gram

force [Taylor, 1949] in *soft* areas. Hardness decreasing below values for calcite and unreacted cement implies the surface has been chemically altered and has become less stiff. This hardness decrease (HV= 23 in the softest of areas) and the weight % decrease in portlandite from XRD data, coupled with the gradual decrease in aperture are consistent with the fracture having become more compressible (Figure 3.2).

Changes in physical appearance of cement reacted with brine suggests the fracture surface composition has been altered. XRD data shows the highest increase of calcite was seen in the *hard* regions. SEM imaging of these areas shows large sheet-like formations/crystals that develop, and EDX spectra show calcium as the predominant element (Figure 3.8). These results indicate that the fluid initially flows along the entire interface until calcite precipitates and creates preferential pathways furthering alteration in the flowpath (*soft*).

Figure 3.9 shows physical appearance of the *soft* regions, which were reacted with saline brine, and provides evidence that the fracture in that area has been altered. XRD data identifies that portlandite is almost absent in surface composition, and the EDX spectra identifies new elements (e.g. iron, aluminum, and magnesium) that are constituents of the carbon steel that had not been seen in either unreacted or de-ionized reacted analyses. This indicates that not only does the saline brine strip the calcium from portlandite, but it also corrodes the steel and deposits this corroded material along the fracture. Deposits of corroded material are seen in Figure 3.2 (orange matter). The corrosion of the steel may be why the *soft* areas are different in appearance when comparing to images taken from

unreacted cement and fracture surfaces reacted with de-ionized water. BR sample has unique crystal structures and shapes that were not seen in unreacted and DI samples (Figure 3.9).

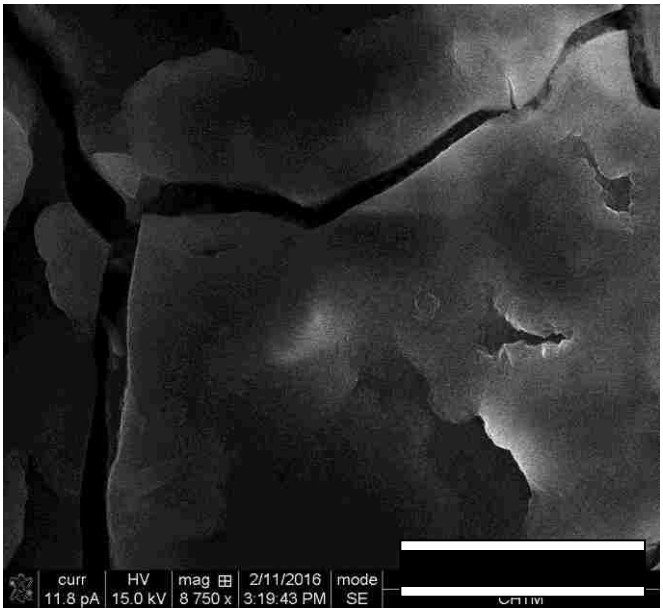
curr
11.8 pA
HV
15.0 kV
mag
8 750 x
2/11/2016
3:19:43 PM
mode
SE

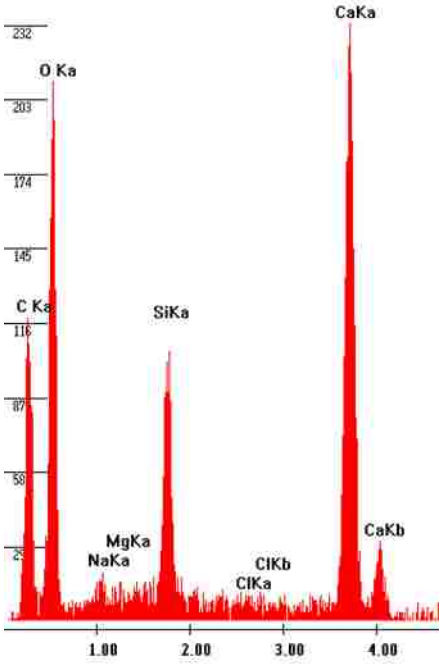
CaKa
O Ka
C Ka
SiKa
MgKa
NaKa
ClKb
ClKa
CaKb
1.00
2.00
3.00
4.00

[redacted]

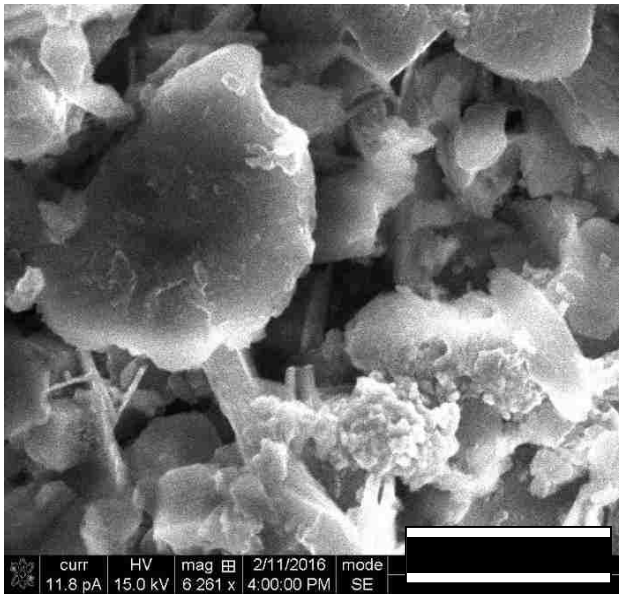
curr
11.8 pA
HV
15.0 kV
mag
6 261 x
2/11/2016
4:00:00 PM
mode
SE

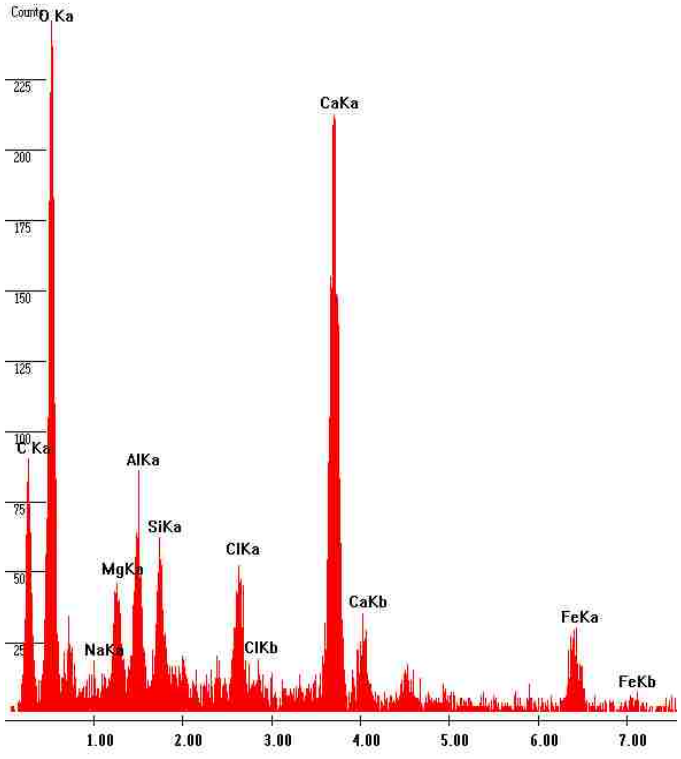
Counts
O Ka
CaKa
C Ka
AlKa
SiKa
ClKa
MgKa
CaKb
FeKa
NaKa
ClKb
FeKb
225
200
175
150
125
100
75
50
25
1.00
2.00
3.00
4.00
5.00
6.00
7.00

[redacted]

Chapter 4

Conclusions

4.1 Research Conclusions

After initial plastic deformation of the fracture surface, cyclic stresses caused an elastic response of the hydraulic aperture. The hydraulic aperture did not exhibit plastic deformation in subsequent stress cycles after reactions between cement and de-ionized water and brine occurred.

The decrease of hardness in the fractured cement system was caused by the dissolution of portlandite and the precipitation of calcite when exposed to both flow of de-ionized water and brine at a pressure of 400 kPa. Quantitative analyses of XRD patterns suggest that the lowest content of portlandite was observed in areas where micro-hardness measurements were lowest after reaction of fractured cement with both deionized water and brine solutions. Even though hardness had decreased in areas where high calcite content was observed, it was where portlandite had decreased most that it yielded the lowest values for hardness. The hardness decrease seen in DI and BR was similar to findings of Walsh et al. (2014) Kutchko et al. (2007) who found acidic brines to decrease and inherently the hardness and strength of cement.

Hydraulic aperture data is indicative that a “self-healing” effect occurs when fractured cement is reacted with brine. The flow of de-ionized water through fractured cement at a pressure of 400 kPa resulted in a hydraulic aperture of 23 μm, which is one order of

magnitude greater than the equivalent hydraulic aperture obtained for intact cement (2 µm). Flow of brine through fractured cement, however, resulted in a hydraulic aperture of 6µm, which is within the same order of magnitude for equivalent hydraulic aperture for intact cement (2 µm). This closure - occurring in conjunction with a loss of calcium from the injected solution, reduced hardness, the increased calcite shown in XRD analysis, and the fact the two cement halves were stuck together at the end of testing -shows that calcium precipitation/dissolution serves as a main role in healing/closing the fracture. A non-acidic brine has shown to induce the same self-healing effects that were seen with an acidic-brine in the studies of Huerta et al. (2011, 2012) and Abdoulghafour et al. (2014).

With flow of de-ionized water and brine, hydraulic apertures on fractured cement decrease over time under sustained confinement. Under a load of 11 MPa and constant injection of both deionized water and brine solutions, hydraulic aperture measurements showed a gradual decrease. This confirms that as portlandite decreases within cement, so do the mechanical properties and this allows for the fracture to be more compressible.

The objective of this study was met by characterizing the physical-chemical response of a fracture in cement that is reacted with de-ionized water and a non-acidic brine. Potential communication of saline aquifers and freshwater aquifers is better understood in the fact that a saline brine flowing through a fractured wellbore sheath can provide a self-healing effect to the fracture.

4.2 Future Work

This study revealed that the alteration of fractured wellbore cement is a function of time. Flow of brine and/or water for durations longer than used in the current study may continue to reduce the hydraulic aperture of the fracture through additional precipitation and/or stiffness reduction of the cement adjacent to the fracture. Longer duration testing would provide evidence of the ultimate or final state that may develop under field conditions.

Tests with a greater injection pressure would provide insight on how calcite precipitation would withstand hydraulic forces imposed by fluids traveling faster through the fracture. Higher temperature fluid flowing through fractures would be more consistent with *in situ* conditions and further detail the role of dissolution/precipitation reactions that were seen.

Bibliography

Abdoulghafour, H., Luquot, L., & Gouze, P. (2013). Characterization of the mechanisms controlling the permeability changes of fractured cements flowed through by CO_2-rich brine. *Environmental science & technology*, *47*(18), 10332-10338.

Agostini, F., Lafhaj, Z., Skoczylas, F., & Loodsveldt, H. (2007). Experimental study of accelerated leaching on hollow cylinders of mortar. *Cement and concrete research*, *37*(1), 71-78.

Baur, I., Keller, P., Mavrocordatos, D., Wehrli, B., & Johnson, C. A. (2004). Dissolution-precipitation behaviour of ettringite, monosulfate, and calcium silicate hydrate. *Cement and concrete research*, *34*(2), 341-348.

Brondel, D., Edwards, R., Hayman, A., Hill, D., Mehta, S., & Semerad, T. (1994). Corrosion in the oil industry. *Oilfield review*, *6*(2), 4-18.

Brufatto, C., Cochran, J., Conn, L., Power, D., El-Zeghaty, S. Z. A. A., Fraboulet, B. & Levine, J. R. (2003). From mud to cement—building gas wells. *Oilfield Review*, 15(3), 62-76.

Brunet, J. P. L., Li, L., Karpyn, Z. T., & Huerta, N. J. (2016). Fracture opening or self-sealing: Critical residence time as a unifying parameter for cement–CO_2–brine interactions. *International Journal of Greenhouse Gas Control*, *47*, 25-37.

Brunet, J. P. L., Li, L., Karpyn, Z. T., Kutchko, B. G., Strazisar, B., & Bromhal, G. (2013). Dynamic evolution of cement composition and transport properties under conditions relevant to geological carbon sequestration. *Energy & Fuels*, *27*(8), 4208-4220.

Carde, C., Escadeillas, G., & François, A. H. (1997). Use of ammonium nitrate solution to simulate and accelerate the leaching of cement pastes due to deionized water. *Magazine of Concrete Research*, *49*(181), 295-301.

Carde, C., & Francois, R. (1999). Modelling the loss of strength and porosity increase due to the leaching of cement pastes. *Cement and Concrete Composites*, 21(3), 181-188.

Carey, J. W., Svec, R., Grigg, R., Zhang, J., & Crow, W. (2010). Experimental investigation of wellbore integrity and CO 2–brine flow along the casing–cement microannulus. *International Journal of Greenhouse Gas Control*, *4*(2), 272-282.

Carey, J. W., Lewis, K., Kelkar, S., & Zyvoloski, G. A. (2013). Geomechanical Behavior of Wells in Geologic Sequestration. *Energy Procedia*, 37, 5642-5652.

Carroll, S., Carey, J. W., Dzombak, D., Huerta, N. J., Li, L., Richard, T. & Zhang, L. (2016). Review: Role of chemistry, mechanics, and transport on well integrity in CO_2 storage environments. *International Journal of Greenhouse Gas Control*, 49, 149-160.

Choi, Y. S., Young, D., Nešić, S., & Gray, L. G. (2013). Wellbore integrity and corrosion of carbon steel in CO_2 geologic storage environments: A literature review. *International Journal of Greenhouse Gas Control*, *16*, S70-S77.

Conley, S., Franco, G., Faloona, I., Blake, D. R., Peischl, J., & Ryerson, T. B. (2016). Methane emissions from the 2015 Aliso Canyon blowout in Los Angeles, CA. *Science*, 351(6279), 1317-1320.

De Andrade, J., Torsæter, M., Todorovic, J., Opedal, N., Stroisz, A., & Vralstad, T. (2014, March). Influence of casing centralization on cement sheath integrity during thermal cycling. In IADC/SPE Drilling Conference and Exhibition. Society of Petroleum Engineers.

Dusseault, M. B., Gray, M. N., & Nawrocki, P. A. (2000, January). Why oilwells leak: cement behavior and long-term consequences. In International Oil and Gas Conference and Exhibition in China. Society of Petroleum Engineers.

Gasda, S. E., Bachu, S., & Celia, M. A. (2004). Spatial characterization of the location of potentially leaky wells penetrating a deep saline aquifer in a mature sedimentary basin. *Environmental geology*, *46*(6-7), 707-720.

Han, J., Zhang, J., & Carey, J. W. (2011). Effect of bicarbonate on corrosion of carbon steel in CO_2 saturated brines. *International Journal of Greenhouse Gas Control*, 5(6), 1680-1683.

Hassanizadeh, S. M., & Gray, W. G. (1987). High velocity flow in porous media. Transport in porous media, 2(6), 521-531.

Heathman, J. F., & East Jr, L. E. (1992, January). Case histories regarding the application of microfine cements. In *SPE/IADC Drilling Conference*. Society of Petroleum Engineers.

Huerta, N. J., Bryant, S. L., Strazisar, B. R., & Hesse, M. (2011). Dynamic alteration along a fractured cement/cement interface: Implications for long term leakage risk along a well with an annulus defect. *Energy Procedia*, 4, 5398-5405.

Huerta, N. J., Hesse, M. A., Bryant, S. L., Strazisar, B. R., & Lopano, C. L. (2012). Experimental evidence for self-limiting reactive flow through a fractured cement core: Implications for time-dependent wellbore leakage. *Environmental science & technology*, 47(1), 269-275.

Haluszczak, L. O., Rose, A. W., & Kump, L. R. (2013). Geochemical evaluation of flowback brine from Marcellus gas wells in Pennsylvania, USA. *Applied Geochemistry*, 28, 55-61.

Huitt, J. L. (1956). Fluid flow in simulated fractures. *AIChE Journal*, *2*(2), 259-264.

Jain, J., & Neithalath, N. (2009). Analysis of calcium leaching behavior of plain and modified cement pastes in pure water. *Cement and Concrete Composites*, 31(3), 176-185.

Kutchko, B. G., Strazisar, B. R., Dzombak, D. A., Lowry, G. V., & Thaulow, N. (2007). Degradation of well cement by CO_2 under geologic sequestration conditions. *Environmental science & technology*, 41(13), 4787-4792.

Lavrov, A., Torsæter, M., Albawi, A., Todorovic, J., Opedal, N., & Cerasi, P. (2014, August). Near-well integrity and thermal effects: a computational road from laboratory to field scale. In 48th US Rock Mechanics/Geomechanics Symposium. American Rock Mechanics Association.

Loosveldt, H., Lafhaj, Z., & Skoczylas, F. (2002). Experimental study of gas and liquid permeability of a mortar. *Cement and Concrete Research*, 32(9), 1357-1363.

Marchand, J., Bentz, D. P., Samson, E., & Maltais, Y. (2001). Influence of calcium hydroxide dissolution on the transport properties of hydrated cement systems. Reactions of calcium hydroxide in concrete. Westerville, OH: *American Ceramic Society*, 113-129.

Marty, N. C., Tournassat, C., Burnol, A., Giffaut, E., & Gaucher, E. C. (2009). Influence of reaction kinetics and mesh refinement on the numerical modelling of concrete/clay interactions. *Journal of Hydrology*, *364*(1), 58-72.

Mason, H. E., Du Frane, W. L., Walsh, S. D., Dai, Z., Charnvanichborikarn, S., & Carroll, S. A. (2013). Chemical and mechanical properties of wellbore cement altered by CO_2-rich brine using a multianalytical approach. *Environmental science & technology*, 47(3), 1745-1752.

Nygaard, R., Salehi, S., Weideman, B., & Lavoie, R. G. (2014). Effect of dynamic loading on wellbore leakage for the wabamun area CO_2-sequestration project. *Journal of Canadian Petroleum Technology*, 53(01), 69-82.

Oliver, W. C., & Pharr, G. M. (1992). An improved technique for determining hardness and elastic modulus using load and displacement sensing indentation experiments. *Journal of materials research*, *7*(06), 1564-1583.

Skoczylas, F. (2005). Multiphysics processes in concrete. *Revue européenne de génie civil*, *9*(5-6), 597-618.

Sobolik, S. R., & Ehgartner, B. L. (2006). Analysis of Salt and Casing Fracture Mechanisms During Cavern Integrity Testing for SPR Salt Caverns. SAND2007-1974, Sandia National Laboratories, Albuquerque, New Mexico.

Taylor, E. W. (1949). Correlation of the Mohs's scale of hardness with the Vickers's hardness numbers. *Mineral.* Mag, 28, 718-721.

U.S. Energy Information Administration (EIA), Independent Statistics & Analysis (2015). Cost of Crude Oil and Natural Gas Wells Drilled data set -- dollars (US) -- , 2002 to 2007 [Data set]. Retrieved from http://www.eia.gov/dnav/ng/ng_enr_wellcost_s1_a.html.

Walsh, S. D., Mason, H. E., Du Frane, W. L., & Carroll, S. A. (2014). Mechanical and hydraulic coupling in cement–caprock interfaces exposed to carbonated brine. *International Journal of Greenhouse Gas Control*, 25, 109-120.

Wigand, M., Kaszuba, J. P., Carey, J. W., & Hollis, W. K. (2009). Geochemical effects of CO_2 sequestration on fractured wellbore cement at the cement/caprock interface. *Chemical Geology*, 265(1), 122-133.

Witherspoon, P. A., Wang, J. S. Y., Iwai, K., & Gale, J. E. (1980). Validity of cubic law for fluid flow in a deformable rock fracture. *Water resources research*, 16(6), 1016-1024.

Wiprut, D., & Zoback, M. (2000). Constraining the stress tensor in the Visund field, Norwegian North Sea: Application to wellbore stability and sand production. *International Journal of Rock Mechanics and Mining Sciences*, 37(1), 317-336.

Yurtdas, I., Xie, S. Y., Burlion, N., Shao, J. F., Saint-Marc, J., & Garnier, A. (2011). Influence of chemical degradation on mechanical behavior of a petroleum cement paste. *Cement and Concrete Research*, 41(4), 412-421.

Zhang, M., & Bachu, S. (2011). Review of integrity of existing wells in relation to CO_2 geological storage: What do we know*? International Journal of Greenhouse Gas Control*, 5(4), 826-840.

Zhang, J., Martin, F.J., 2011. Corrosion of carbon steel by carbonate–bicarbonate solution for CO_2 capture. Los Alamos National Laboratory internal report and personal communication.